




A Variable Scheduling Maintenance Culture Platform for Mammalian Cells

SLAS Technology
2021, Vol. 26(2) 209–217
© The Author(s) 2020



DOI: 10.1177/2472630320972109
journals.sagepub.com/home/jla



Koji Ochiai^{1*}, Naohiro Motozawa^{2,3*}, Motoki Terada²,
Takaaki Horinouchi^{1,4} , Tomohiro Masuda², Taku Kudo⁵,
Motohisa Kamei⁵, Akitaka Tsujikawa³, Kenji Matsukuma⁵, Tohru Natsume^{5,6},
Genki N. Kanda^{1,2,5} , Masayo Takahashi^{2,7}, and Koichi Takahashi¹ 

Abstract

Cell culturing is a basic experimental technique in cell biology and medical science. However, culturing high-quality cells with a high degree of reproducibility relies heavily on expert skills and tacit knowledge, and it is not straightforward to scale the production process due to the education bottleneck. Although many automated culture systems have been developed and a few have succeeded in mass production environments, very few robots are permissive of frequent protocol changes, which are often required in basic research environments. LabDroid is a general-purpose humanoid robot with two arms that performs experiments using the same tools as humans. Combining our newly developed AI software with LabDroid, we developed a variable scheduling system that continuously produces subcultures of cell lines without human intervention. The system periodically observes the cells on plates with a microscope, predicts the cell growth curve by processing cell images, and decides the best times for passage. We have succeeded in developing a system that maintains the cultures of two HEK293A cell plates with no human intervention for 192 h.

Keywords

mammalian cell culture, growth prediction, LabDroid, variable scheduling automation

Introduction

Culturing cells and tissues is an indispensable part of basic cell biology research and clinical applications, such as cell-based drug screening and transplantation of retinal pigment epithelial cells differentiated from induced pluripotent stem cells¹ in regenerative medicine. Advancements in cell engineering technologies will undoubtedly cause the types and quantities of cells required to increase dramatically. Efficiently producing high-quality cells that become the raw materials for tissues and organs used in regenerative medicine is one of the most important issues for the standardization and dissemination of regenerative medicine. In cell culturing and manufacturing, the heterogeneity of cells and perturbation during manipulation are among the numerous uncertainties that remain.² Previous studies^{3,4} have emphasized the importance of considering such intricate characteristics to ensure the quality of the processed cells. An additional factor to consider is the transfer of tacit knowledge. Such transfer is often inefficient and problematic. It normally results in high education costs and usually serves as an obstacle to standardization and dissemination of regenerative medicine. This knowledge transfer problem poses a serious bottleneck in achieving a well-crafted cell

production workflow outside of the lab to reach the scale of production that clinical applications require.

¹Laboratory for Biologically Inspired Computing, RIKEN Center for Biosystems Dynamics Research, Suita, Osaka, Japan

²Laboratory for Retinal Regeneration, RIKEN Center for Biosystems Dynamics Research, Chuo-ku, Kobe, Hyogo, Japan

³Department of Ophthalmology and Visual Sciences, Kyoto University Graduate School of Medicine, Sakyo-ku, Kyoto, Japan

⁴Laboratory for Multiscale Biosystem Dynamics, RIKEN Center for Biosystems Dynamics Research, Suita, Osaka, Japan

⁵Robotic Biology Institute Inc., Koto-ku, Tokyo, Japan

⁶Department of Life Science and Biotechnology, Cellular and Molecular Biotechnology Research Institute, National Institute of Advanced Industrial Science and Technology (AIST), Koto-ku, Tokyo, Japan

⁷VisionCare Inc., Chuo-ku, Kobe, Hyogo, Japan

*These authors contributed equally.

Received July 2, 2020, and in revised form Oct 8, 2020. Accepted for publication Oct 14, 2020.

Supplemental material is available online with this article.

Corresponding Author:

Koichi Takahashi, Laboratory for Biologically Inspired Computing, RIKEN Center for Biosystems Dynamics Research, 6-2-3 Furuedai, Suita, Osaka 565-0874, Japan.

Email: ktakahashi@riken.jp

To overcome the scalability problems in cell production, various automated culture systems have been developed. Most automated culture systems fall into one of two categories: specialized and multipurpose. Specialized systems aim to scale the quantity of cells produced (capacity), and multipurpose systems aim to scale the types of cells that can be produced (capability). Specialized systems often have fixed configurations and usages and generally feature high-throughput and operational stability. Some examples of this type of machinery include sealed-vessel culture systems that have aseptic spaces for cell cultures that remain unopened during operation.⁵⁻⁸ Robotic arm-assisted systems that utilize articulated robots for autonomous operation are another example.⁹⁻¹⁵ One drawback of specialized systems is that the addition or modification of experimental instruments and procedures poses certain challenges. Because of this lack of flexibility, specialized automated culture systems are generally ill-suited for basic research as the addition of new experiments, the modification of protocols, and the addition of new laboratory equipment are frequently required. Another drawback is that these systems cannot handle many types of cells at once, thus not scaling well for diverse types of cells. Multipurpose systems, on the other hand, allow flexible changes in workflow and the procurement of additional equipment. In addition, these systems can handle multiple samples at once. This advantage makes these systems suitable for scalability problems of cell types. Automated liquid handling workstations,^{16,17} in use for decades in various applications downstream of cell culture processes such as high-throughput screening, represent one such example. Attempts have been made to extend their use into other areas, including maintenance passages of cell culture, phenotyping, genotyping, drug screening, and other cell biology experiments.¹⁸⁻²¹ Recent advancements in mechatronics have made possible the application of industrial-grade human-like dual-arm robots to the automation of various types of experiments in proteomics, drug screening for osteosarcoma, gas chromatography-mass spectrometry (GC-MS) analysis, and chromatin immunoprecipitation analysis.²²⁻²⁵ One significant advantage of utilizing humanoid robots for automating laboratory experiments is that such robots can use the same laboratory equipment as humans. This leads to some significant advantages over other systems. First, the seamless linkage between cell culturing and its downstream processes provides an acceleration of research and development. For example, Fleischer et al. have successfully combined a dual-arm robot with GC-MS that provides a seamless flow from sample preparation to sample transfer to the analyzer and autonomous analysis.²⁴ Second, they facilitate the transfer of tacit knowledge and skills, which is critically important for yielding high-quality results in certain procedures, especially in cell culture.²³

Cell culture experiments consist of an array of processes, including observation, measurement, and passage,

and require various types of equipment. Cell culturing usually takes weeks to months, and the inaccuracies and workload that are inherent through the use of human operators often complicate the process. Conventional systems need complicated and expensive transportation systems to combine various types of equipment and to operate them independently for experiments of long durations, and many of these systems still entrust such transportation procedures to human operators. Cell culturing also involves decision-making and parameter adjustments such as passage timing and reagent addition based on the conditions and evaluation of cell growth. Small-lot multiproduction manufacturing in the industrial field—including assembling IT products such as cell phones, televisions, and computers—has features similar to those encountered in cell culture experiments: complex tasks involving multiple different machines. This area of automation often uses dual-arm robots as well.^{26,27}

In this study, we developed an autonomous variable scheduling cell culture system based on LabDroid, a versatile dual-arm experimental robot,²³ combined with AI-aided fully automated cell growth evaluation and passage timing determination (**Fig. 1**). We demonstrate the performance of the system in culturing human embryonic kidney (HEK293A) cells. This variable scheduling system enables us to maintain multiple cell plates without any human assistance.

Materials and Methods

Definition of Terms

Movement: The smallest action unit for LabDroid to operate. The movement is specified by the joint angle of each arm. For the user, comprehending the movement of the robot from the joint angle values alone is hard. **Command:** A group of actions such as moving plates, transferring reagents, and aspirating media, among others. A command consists of one or more movements. **Job:** The instructions that a user gives LabDroid at one time. A job consists of one or more commands. For example, an observation job consists of opening the door of a CO₂ incubator, holding the target plate, moving the plate, etc.

LabDroid Maholo Including Peripheral Equipment

LabDroid, along with peripheral equipment, was placed inside of a booth consisting of acrylic walls and a stainless steel frame with fan filter units (FFUs; CF-H040, KEYENCE, Osaka, Japan). Air supplied to the platform was cleaned with a top-mounted FFU with HEPA filters to maintain cleanliness. The LabDroid booth consisted of the following equipment: dual-arm robot (YASKAWA Electric Corp., Fukuoka, Japan), refrigerator (CN-25C, Mitsubishi

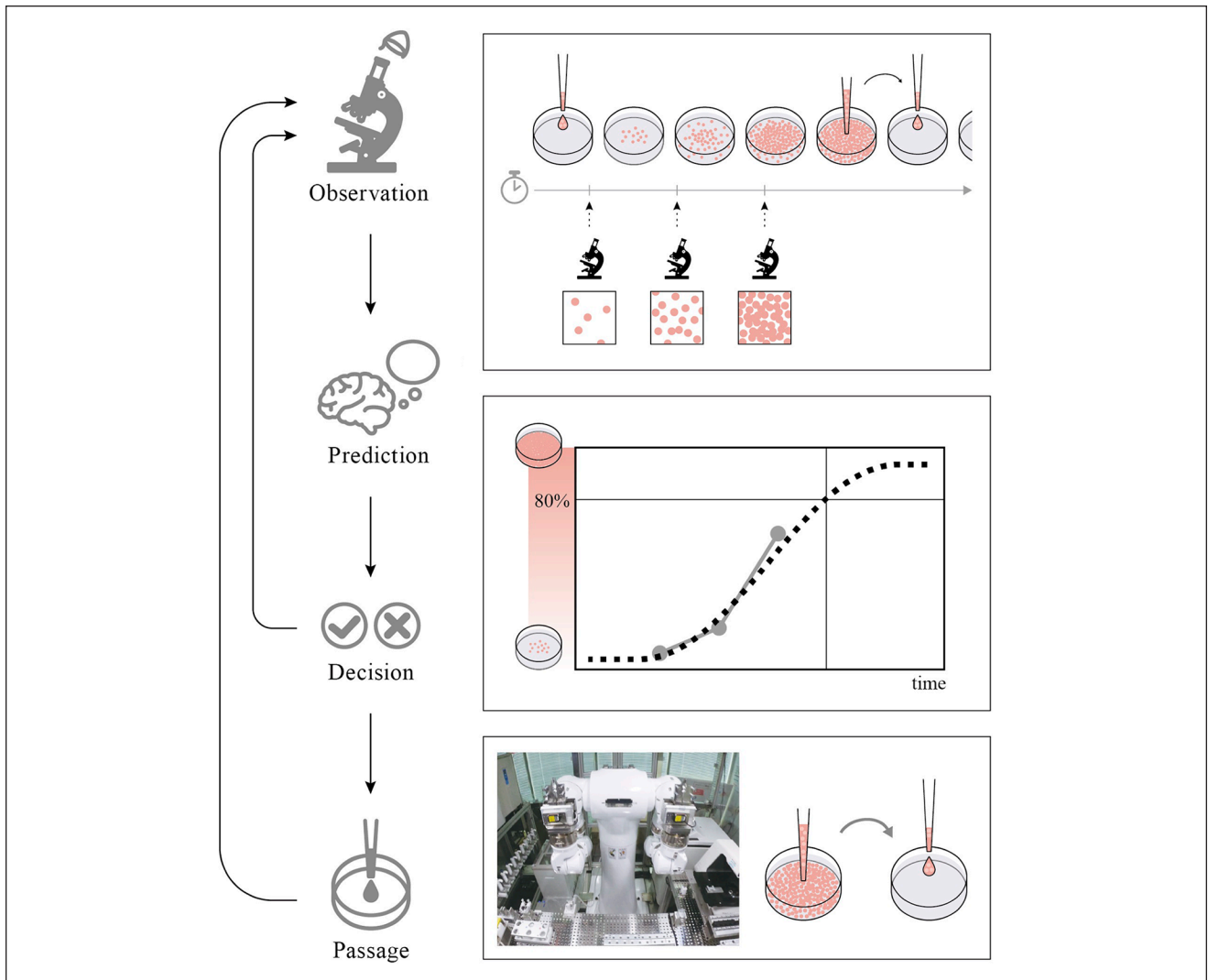


Figure 1. Overall workflow of the developed system. In manual cell culture, cells are observed under a microscope as appropriate, and the cells are replated by performing a passage operation once a certain cell density is reached. To automate these operations, we developed a variable scheduling maintenance culture platform that observes cells every 12 h, predicts the time at which cells will grow to a specified cell density, and executes passage operations by combining LabDroid and software.

Electric Engineering Co., Ltd., Tokyo, Japan), CO₂ incubator (APC-30D, ASTEC Co., Ltd., Fukuoka, Japan), pipette tips (3512-05-HR/3511-05-HR/94410313/94410713/9405 2550, Thermo Fisher Scientific, Waltham, MA), micropipettes (4641110N/4641030N/4641230N/4641210N, Thermo Fisher Scientific), 50 mL tube rack (Robotic Biology Institute Inc., Tokyo, Japan), four 6-well plate rack (Robotic Biology Institute Inc.), dry bath (EC-40RA, AS ONE Corporation, Osaka, Japan), tip sensor (Robotic Biology Institute Inc.), aspirator (SP-30, Air Liquide, Milano, Italy), dust bin (EPD3S, Sekisui Techno Molding Co., Ltd., Tokyo, Japan), and microscope (EVOS FL Auto 2, Thermo Fisher Scientific).

ProtocolMaker (YASKAWA Electric Corp.), software fused for operating LabDroid, allows a user to construct

LabDroid programs with a graphical user interface. The user may specify various settings, such as the origin and destination of tubes and plates, the amount, and the position, as well as the number of suction and dispensation counts for liquid transfer from tubes to plates, the suction and dispensation heights within a tube or plate, the inclination of a plate, and the speed of suction and dispensation.

There is a space to position tubes and plates in front of the LabDroid, and culture operations are performed by moving cell plates, reagents, and labware to the designated locations. LabDroid uses its various sensors to determine if a scheduled operation has been successful. It uses the laser distance sensors embedded in its arms (Suppl. Fig. S1A) when opening and closing the caps of tubes, and the tip sensor (Suppl. Fig. S1B) when attaching and removing a

pipette tip. If the scheduled operation is unsuccessful, an error is reported before reattempting the same operation. When LabDroid fails to execute the operation for the second time, the operation aborts. We registered the shapes and sizes of six-well plates (353046, Corning, Corning, NY) and 50 mL tubes (MS-58500, Sumitomo Bakelite Co., Ltd., Tokyo, Japan) in the system and calibrated location information and actual movements at the time of the LabDroid environment setup. Microscopy images were acquired by running a program created with ProtocolMaker, which orders LabDroid to transfer the cell plates within the CO₂ incubator to the microscope. Using the software supplied with the microscope enabled us to align the imaging of the six-well plates prior to the experiment. Use of a protocol of 26 central tiling images with a 4× objective lens to capture approximately 40% of the well base area enabled the capture of the same position over time, which was also used for image analysis.

Software: Batch Timing Manager

In this experiment, we divided the HEK293A cell line into two plates and cultured them in parallel. The first plate is named “cell plate 1” and the second plate is named “cell plate 2.” The batch timing manager (BTM) manages when and which cell plate to observe and the time of passage. A system initializes the scheduled observation time (SOT) and scheduled passage time (SPT) when the user starts the system. For the first cell plate, the SOT is set to 1 min after initialization and the SPT is set to 1 day after initialization. For the second cell plate, the SOT is set to 30 min after initialization and the SPT is set 1 day and 30 min after initialization. At the scheduled time, the BTM instructs LabDroid to observe or passage the target cell plate.

After the observation, the BTM calculates the density from new microscopy images using the cell density calculator (CDC) and saves the observation time and cell density values to a log file. If the log file has two or more density values for the target cell plate, BTM applies a growth curve predictor (GCP) to the log. Then, the time in which the predicted cell density value will exceed a predetermined value is calculated and set as the new SPT. The SOT is set to 12 h after the last observation or passage. When the schedule includes more than one job at the same time, observation takes precedence over passage, and cell plate 1 takes precedence over cell plate 2.

Software: Cell Density Calculator

We used tiled microscopy images (Suppl. Fig. S2A) to construct cell images and adjusted the microscopic field size to cover as much of the area as possible without showing the edges of the well (Suppl. Fig. S2B). The CDC calculates cell density following eq 1:

$$C = \frac{f(A_c \cap A_i)}{f(A_i)}, \quad (1)$$

where C is the cell density, A_c is the cell area that the program recognizes as being cells (Suppl. Fig. S2C), A_i is the well area, and f is a function that converts area to a pixel count.

The method used for cell area detection is as described by MathWorks²⁸ except for our method using the Canny algorithm in place of the Sobel algorithm for edge detection.²⁹

Software: Growth Curve Predictor

The GCP predicts cell density by fitting the logistic differential equation.³⁰ We defined the logistic function as

$$N_{t+1} = f(N_0, \Delta t, r, K) = \frac{(1 + e^{r\Delta t})N_0}{1 + \frac{a}{K}N_0}, \quad (2)$$

where N_0 is the initial cell count, Δt is the elapsed time from the initial cell count, r is the growth rate, and K is the maximum cell count.

N_0 and r are determined by minimizing the loss calculated as

$$l = \sum_{t=0}^T \left\{ W_p(p_t) \times W_o(o_t) \times \left(N_t - f(N_{p_t}, \Delta t_{p_t}, r, K) \right)^2 \right\}, \quad (3)$$

$$W_p(p_t) = \alpha^{(p_c - p_t)},$$

$$W_o(o_t) = \beta^{(o_c - o_t)},$$

where N_t is the observed density at time t , p_t is the number of passages at time t , p_c is the current number of observations, o_t is the number of observations at time t , o_c is the current number of observations, N_{p_t} is the initial cell density when the number of passages is p_t , and Δt_{p_t} is the time from the last passage when the number of passages is p_t . In other words, the GCP optimizes the initial cell densities for each passage period. This formula is a kind of weighted least squares.³¹ We empirically fixed α to 0.1, β to 1, and K to 1. The GCP applies the Nelder–Mead method³² to eq 3 for function minimization. One limitation of this approach is that it may provide a local minimum rather than the desired global minimum. To circumvent this limitation, the initial values of N_0 and r are sampled 50 times from a

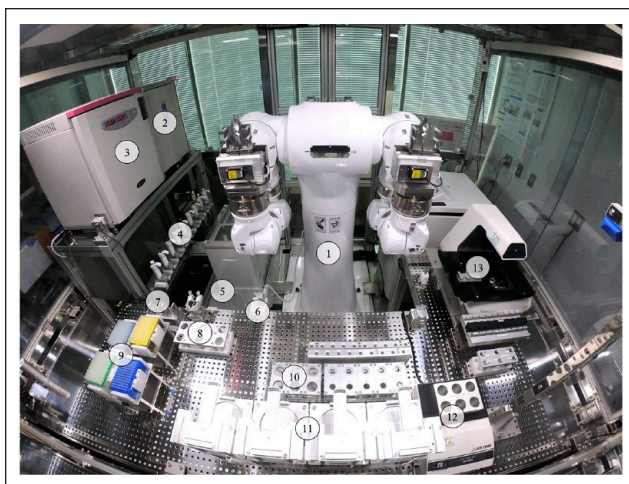


Figure 2. LabDroid Maholo including peripheral equipment. A bird's-eye view of the LabDroid booth: (1) dual-arm robot, (2) refrigerator, (3) CO₂ incubator, (4) micropipettes, (5) dust bin, (6) aspirator, (7) tip sensor, (8) 50 mL tube subrack, (9) pipette tips, (10) 50 mL tube main rack, (11) six-well plate rack, (12) dry bath, and (13) microscope.

uniform distribution ranging from 0.01 to 0.2 and from 0.1 to 2, respectively. If a newly sampled value for N_0 and r yields a smaller loss than that on the first try, N_0 and r are updated to the new value.

Software: Robot Job Manager

The robot job manager (RJM) assembles appropriate jobs from the job library according to the remaining amounts of reagents and/or labware for LabDroid to perform the appropriate operation.

The RJM manages the positions of tubes and plates using a tree data structure, referred to as the supply management model (SMM). The system obtains the initial positions of reagent tubes and plates from the user as a form of SMM. The user then places tubes and plates on the robot workspace (LabDroid booth; see **Fig. 2**).

The RJM assembles jobs sent to LabDroid using batch design, the job library, and the SMM. The user prepares the batch design and job library, and they remain unchanged during control. A batch design is an ordered list of jobs for observation or passage, and the job library is a list of jobs. Some jobs in a batch design may have unspecified details, such as having no source position for the new plate. However, all jobs in the job library have detailed instructions. When sending jobs for observation or passage, the program uses the SMM to first search for executable jobs from the job library. It then replaces some jobs in the batch design with executable jobs in the job library. After this replacement, all jobs in the batch design become executable. This executable job list is referred to as an assembled batch.

When ordering LabDroid to run an observation job, the RJM first finds the position of the cell plate to be observed from the SMM. Next, the RJM makes and sends the assembled batch to LabDroid. When ordering LabDroid to run a passage job, the RJM first determines the position of the cell plate to be passaged from the SMM. Then, it finds the new plate and remaining reagents needed for passage. Afterward, the program calculates the amount of plates and reagent to be used in the passage and reflects this amount in the SMM. Finally, the RJM makes and sends the assembled batch to LabDroid.

Software: Dashboard

The Dashboard is an HTML-based monitoring system to allow humans to observe the progress of a process. The system displays the following information: (1) LabDroid status (running or halted)—LabDroid status is presented as running when less than 30 min has elapsed since the latest run time and halted otherwise; (2) scheduled time—the SOT and SPT of each line; (3) observed cell density and growth curve—plot of calculated cell density and fitted lines estimated after the latest passage; and (4) job order list—the names of the jobs sent to LabDroid, their time stamps, and execution validity (whether LabDroid successfully concluded the process or not).

Preparation of Reagents and Labware

We imported all other reagents and labware into the LabDroid booth as shown in **Supplemental Table S1**. We prepared phosphate-buffered saline (PBS), trypsin, and Dulbecco's modified Eagle medium (DMEM) in 50 mL tubes and placed them in the refrigerator; then we prepared two bottles of DMEM. When the remaining amount of the first bottle fell below a specified value, the second bottle was used. We incubated cells in No. 1 and No. 5 container racks in the CO₂ incubator and placed eight 6-well plates in the CO₂ incubator. Users determined the order of use. We prepared ethanol (326-00031, FUJIFILM Wako Pure Chemical Corp., Osaka, Japan) in 50 mL tubes, placed them in a refrigerator and tube subrack, and used them to clean the inside of the hose by aspirating ethanol after completing the job of handling the medium in the aspirator.

Cell Culture Experiments

We obtained HEK293A cells from Thermo Fisher Scientific (R70507) and maintained them in DMEM (043-30085, FUJIFILM Wako Pure Chemical), supplemented with 10% fetal bovine serum (FBS; 555-21245, Biosera, Nuaille, France), 100 U/mL penicillin-streptomycin (15140-122, Thermo Fisher Scientific), and 2 mM L-glutamine (G7513, Sigma-Aldrich, St. Louis, MO) in a humidified atmosphere of 5% CO₂ and 95% air at 37 °C.

Prior to cell culturing with a robot, we prepared cells manually. We seeded cells at the A2 well position in six-well plates, washed them with PBS (10010023, Thermo Fisher Scientific), detached them with 0.05% trypsin (25300054, Thermo Fisher Scientific) by pipetting after 2 min at room temperature, and replated at 1×10^5 and 2×10^5 cells/well. We then transferred the cells to the CO₂ incubator in the LabDroid booth unit and created robot job library files (**Suppl. Table S2**) with ProtocolMaker, confirmed by LabDroid to be correct in advance. Each job library file contains an individual step of passage or observation. The files were then sent to the appropriate folder in the LabDroid control PC. The passage procedure by LabDroid was made according to the human method as set out in **Supplemental Table S3**. Each row of this table describes an individual passage step.

Results and Discussion

LabDroid-Based Autonomous Cell Culture System for Cell Passage

Cell culturing under artificial conditions requires attaching the cells to the flat bottom of a plastic tissue culture dish or the culture dish filled with a liquid medium containing nutrients. When cells proliferate and cell density exceeds a certain level, cells must be passaged onto a new culture dish by detaching adherent cells using enzymes, collecting, and diluting. To maintain healthy cells, the continuation of culturing and passage to maintain the cell density within an appropriate range is necessary.

We developed a variable scheduling robot-AI system that automatically observes growing cells on plates every 12 h with a microscope, predicts the time at which the cell density exceeds the designated level based on the observation, and passages the cells at the optimal timing. The system can culture two cell plates at the same time (**Fig. 1**). The user must set the following initial parameters: (1) initial value of the passage time for the first cell plate, (2) initial value of the passage time for the second cell plate, (3) initial value of the observation time of the first cell plate, (4) initial value of the observation time of the second cell plate, (5) minimum observation interval, (6) minimum gap between joints, and (7) cell density for timing of passage. The user loads reagents and cell plates before starting the operation.

Software Development and Integration

The system consists of a LabDroid robot, a robot job library, and five computer programs. LabDroid is a versatile dual-arm robot for life science experiments with very high positional accuracy.²³ We placed a refrigerator, a CO₂ incubator, and a microscope in addition to other peripherals, such as tube racks, in the LabDroid booth (**Fig. 2**). The protocol

editor software called ProtocolMaker was used to define elementary robot commands such as adding reagents, cell detachment, and transfer of cell suspension (**Suppl. Table S3**), and 31 robot jobs, such as passage and observation, were constructed by assembling the elementary commands (**Suppl. Table S2**).

The software system consists of five components: (1) a BTM, (2) a CDC, (3) a GCP, (4) an RJM, and (5) a graphical dashboard (**Fig. 3**). The BTM runs continuously for the duration of the experiment and manages which cell plate to observe or transfer based on a line table file (**Suppl. Fig. S3A**). The line table file describes the next SOT and the next SPT for each cell plate. The CDC is a program that calculates cell density from microscopy images by the means of image processing and executes each time for a completed observation (**Suppl. Fig. S3B**). The GCP estimates the growth curve of the target cell (**Suppl. Fig. S3C**) and predicts the time in which the cell density exceeds a preset value specified by the user. The RJM generates a sequence of robot commands to execute appropriate operation (observation or passage) while taking into consideration the remaining labware and reagents (**Suppl. Fig. S3D,E**). The dashboard provides a graphical view for the user to monitor the status of the system and cell growth curve via a web browser (**Suppl. Fig. S4**).

The Developed System Automatically Cultured HEK293A Cells

We then used the developed system to maintain a culture of the HEK293A cell line, and selected this cell line for three reasons: (1) its single-cell-layer formation simplifies the image processing required to calculate the cell area, (2) its high adhesion to the bottom of the culture plate alleviates the difficulties in implementation of cell handling via robotic hands, and (3) its fast growth rate eliminates the need to create a media exchange job, as the cells would need to be passaged by the time a media exchange would be necessary.

First, we defined the various operating parameters of LabDroid in the passage process, such as the speed of reagent addition, the angle of the plate during aspiration, and the number of pipetting cycles during cell detachment in accordance with the HEK293A cells (**Suppl. Table S3**). We calculated the cell dilution rate of the cells before and after the passage to be 27%.

We imported two plates with a different number of seeded cells, the reagents required, and consumables into the robot booth, and started the system with the passage target set to 80% cell density. The system operated for 192 consecutive hours, during which the system executed a total of eight passage processes and 39 cell observation processes. Upon completing its operation, the system had executed a total of 95 jobs without yielding any system-derived errors (**Suppl.**

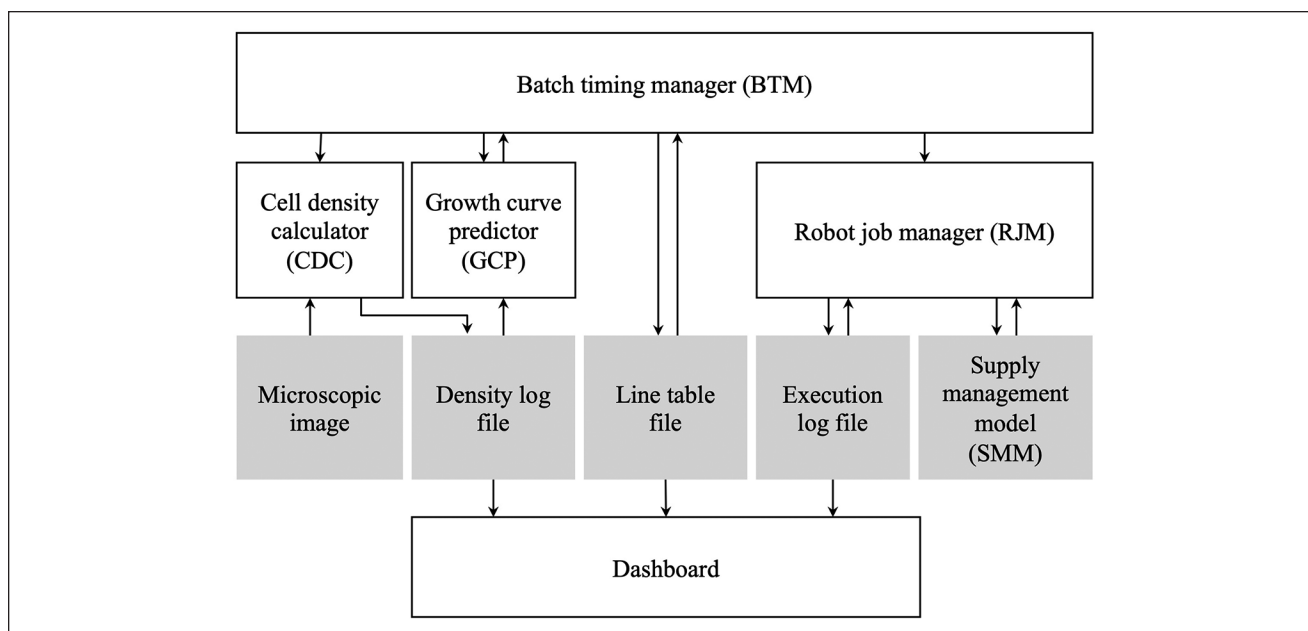


Figure 3. System components. Relationships between components. Black frames represent components, and gray boxes represent files. The density log file is a log of calculated cell density, and the execution log file is a log of jobs sent to LabDroid. The line table file, SMM, and components are described in Materials and Methods.

Table S4A). During the operation, the system automatically performed cell observations every 12 h and calculated changes in cell density over time (**Fig. 4A**, **Suppl. Fig. S5A**, and **Suppl. Table S5A**). The mean (\pm SD) cell density at passage in this experiment was $82.3\% \pm 1.4\%$ ($n = 9$). Of the 95 executed jobs, 45 were executed with the lights out (6:00 p.m. to 6:00 a.m.).

We then changed the passage target to 60% cell density and repeated the same experiment. The system operated for 159 consecutive hours without human intervention or critical system error, conducting a total of seven passage processes and 33 cell observation processes. In total, the system executed 82 jobs and performed 45 of these between 6:00 p.m. and 6:00 a.m. (**Fig. 4B**, **Suppl. Fig. S5B**, and **Suppl. Tables S4B and S5B**). The mean (\pm SD) cell density at passage was $59.8\% \pm 3.7\%$ ($n = 7$). During the second passage for cell plate 2, the system scheduled the observation and passage processes at the same time. As per the protocol defined in the Materials and Methods section, observation took precedence over passage. The system suspended operation three times when it detected defective labware and prompted human operators to exchange such labware at the next available time. This exception handling procedure, however, had no effect on the successful completion of the experiment. No contamination occurred in all experimental periods. The mean time (\pm SD) required for cell observation starting with the removal of the cell plates from the CO₂ incubator and ending with the completion of the cleanup procedure was 7 min and 35 ± 8 s, and the mean (\pm SD) time required for passage was 30 min and 41 ± 9 s.

These times are comparable to manual cell culturing experiments. According to a study that quantified the process of manual culturing experiments using a video-based analysis, the average time required for cell passage was about 35 min.³³ It is certain from experience that the LabDroid is not capable of performing individual operations as quickly as humans can. Therefore, we attempted to shorten the processing time by simplifying the protocol. For example, we omitted the use of a centrifuge while washing the cells prior to passage in our experiment. These modifications to the protocol enabled our system to achieve passage times comparable to those of manual operation.

Supplemental Figure S6 shows the prediction accuracy of the ideal passage timing. The prediction error was close to zero immediately after the passage, and gradually increased as data accumulated over time, although it must be noted that the error decreased just before the next passage. We attribute the increase in prediction error between passages to two reasons: (1) the observed time series of cell density deviated from our logistic function-based prediction model (GCP), and (2) rapid changes in cell density made estimation given by the CDC less accurate. Investigation into the validity of the logistic function-based cell growth model is an issue for future research. For example, the discrepancy between the actual cell growth curve and the mathematical model could have resulted in inaccurate cell growth rate estimations in GCP. The mean (\pm SD) error of ideal passage timing was 1.8 ± 2.3 h ($n = 36$) when the passage target was set to 80% and 0.1 ± 3.0 h ($n = 31$) when the passage target was set to 60%.

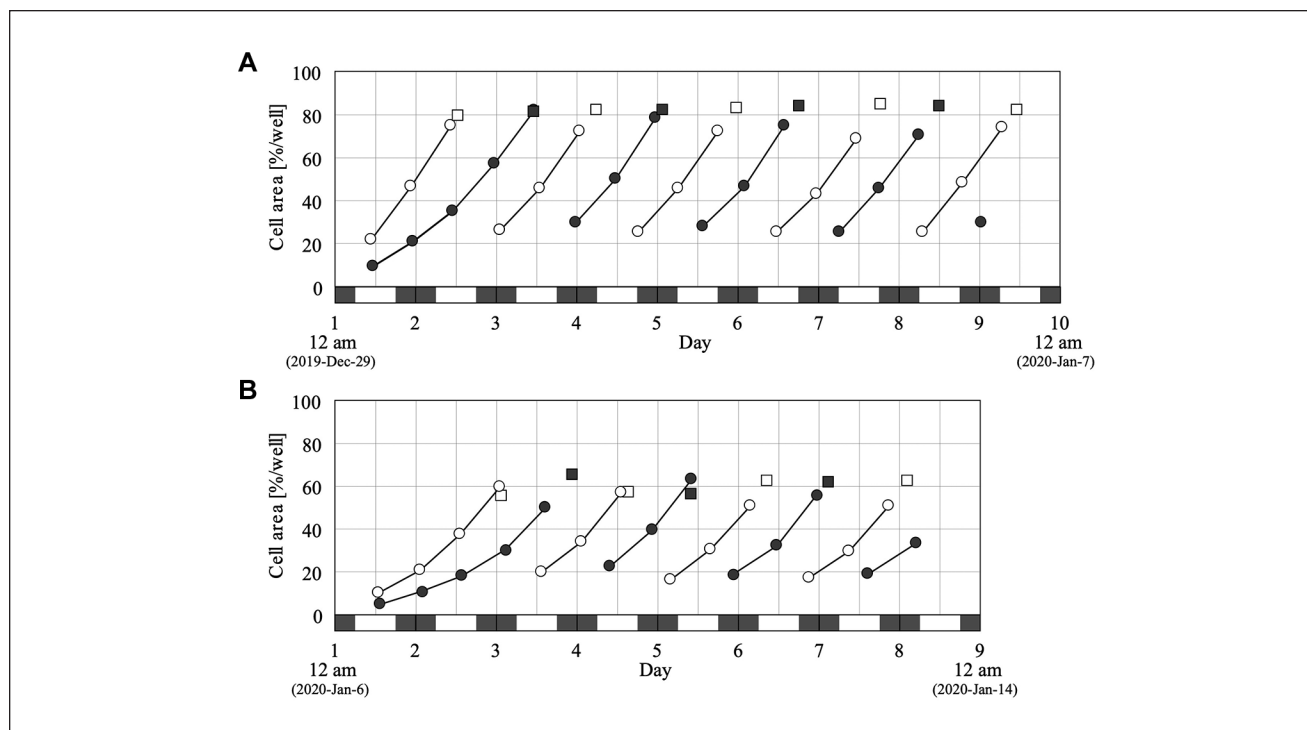


Figure 4. HEK293A cell culture by developed system. HEK293A cells were seeded into six-well plates and cultured by the developed system, which was set to 80% (A) or 60% (B) as a target cell density value. White and black markers represent the data of cell plates 1 and 2. Circles represent the operated time of observation, and squares represent the operated time of passage. White-colored bars on the horizontal axis represent daytime (6:00 a.m. to 6:00 p.m.), and gray-colored-bars on the horizontal axis represent nighttime (6:00 p.m. to 6:00 a.m.).

Outlook

In conclusion, our system succeeded in the autonomous passage of two mammalian cell plates containing a different number of seeded cells simultaneously, with variable target passage cell density values. One limitation of our system is that it changes the single-variable parameter, the timing of passage, solely on the observation and prediction of the cell density. The system has potential for further applications. For example, human experts culture cells not only by estimating cell densities but also by considering some other important factors, such as the 3D cell structure, temporal development, environmental factors, and pH of the media, as well as distinguishing between living and dead cells. The current system assesses only the quantity of growing cells to determine passage timing, but it can perform other procedures, such as discarding cells, expanding cultures, changing media, and freezing and thawing cells based on the quality of the cells along with the quantity. Such extensions have an important potential to culture a wider range of cell types or for adoption in more advanced cell culturing operations, such as differentiation induction.

Acknowledgments

We thank T. Mitsuyama, H. Kiyonari, S. Wada, T. Sakurada, and Y. Ozawa for useful discussions; E. Takagi and H. Hirabayashi for

research support; H. Uchida for illustrations; and J. Freeman for carefully proofreading the manuscript. We also thank all the lab members at RIKEN BDR, in particular, N. Sakai, G. A. Sunagawa, N. Koide, and K. Itaya, for their kind help in preparing the materials, supporting experiments, and useful discussions.

Declaration of Conflicting Interests



The authors declared the following potential conflicts of interest with respect to the research, authorship, and/or publication of this article: T.K., M.K., K.M., T.N., and G.N.K. are employees, executives, or stakeholders of Robotic Biology Institute Inc., which may benefit financially from increased scientific use of LabDroid Maholo. All other authors declare no competing interests.

Funding

The authors disclosed receipt of the following financial support for the research, authorship, and/or publication of this article: This work was supported by a project subsidized by the New Energy and Industrial Technology Development Organization (NEDO, to M. Takahashi), the JST-Mirai Program (JPMJMI18G4, to K.T.), an internal grant from the RIKEN Center for Biosystems Dynamics Research (to M. Takahashi and K.T.), the RIKEN Engineering Network (to M. Takahashi), and the RIKEN Junior Research Associate program (to K.O. and N.M.).

ORCID iDs

Takaaki Horinouchi  <https://orcid.org/0000-0001-9141-9103>

Genki N. Kanda  <https://orcid.org/0000-0002-6372-241X>
Koichi Takahashi  <https://orcid.org/0000-0001-9141-9103>

References

- Mandai, M.; Watanabe, A.; Kurimoto, Y.; et al. Autologous Induced Stem-Cell-Derived Retinal Cells for Macular Degeneration. *N. Engl. J. Med.* **2017**, *376*, 1038–1046.
- Kanie, K.; Sakai, T.; Imai, Y.; et al. Effect of Mechanical Vibration Stress in Cell Culture on Human Induced Pluripotent Stem Cells. *Regen. Ther.* **2019**, *12*, 27–35.
- Kino-oka, M.; Mizutani, M.; Medcalf, N. Cell Manufacturability. *Cell Gene Therapy Insights* **2019**, *5*, 1347–1359.
- Kino-oka, M.; Sakai, Y. Preface of the Special Issue “Cell Manufacturability.” *Regen. Ther.* **2019**, *12*, 1.
- Kino-Oka, M.; Chowdhury, S. R.; Muneyuki, Y.; et al. Automating the Expansion Process of Human Skeletal Muscle Myoblasts with Suppression of Myotube Formation. *Tissue Eng. Part C Methods* **2009**, *15*, 717–728.
- Nishimura, A.; Nakajima, R.; Takagi, R.; et al. Fabrication of Tissue-Engineered Cell Sheets by Automated Cell Culture Equipment. *J. Tissue Eng. Regen. Med.* **2019**, *13*, 2246–2255.
- dos Santos, F. F.; Andrade, P. Z.; da Silva, C. L.; et al. Bioreactor Design for Clinical-Grade Expansion of Stem Cells. *Biotechnol. J.* **2013**, *8*, 644–654.
- Matsumoto, E.; Koide, N.; Hanzawa, H.; et al. Fabricating Retinal Pigment Epithelial Cell Sheets Derived from Human Induced Pluripotent Stem Cells in an Automated Closed Culture System for Regenerative Medicine. *PLoS One* **2019**, *14*, e0212369.
- Konagaya, S.; Ando, T.; Yamauchi, T.; et al. Long-Term Maintenance of Human Induced Pluripotent Stem Cells by Automated Cell Culture System. *Sci. Rep.* **2015**, *5*, 16647.
- Thomas, R. J.; Chandra, A.; Hourd, P. C.; et al. Cell Culture Automation and Quality Engineering: A Necessary Partnership to Develop Optimized Manufacturing Processes for Cell-Based Therapies. *JALA J. Assoc. Lab. Autom.* **2008**, *13*, 152–158.
- Liu, Y.; Hourd, P.; Chandra, A.; et al. Human Cell Culture Process Capability: A Comparison of Manual and Automated Production. *J. Tissue Eng. Regen. Med.* **2010**, *4*, 45–54.
- Soares, F. A. C.; Chandra, A.; Thomas, R. J.; et al. Investigating the Feasibility of Scale Up and Automation of Human Induced Pluripotent Stem Cells Cultured in Aggregates in Feeder Free Conditions. *J. Biotechnol.* **2014**, *173*, 53–58.
- Lehmann, R.; Gallert, C.; Roddelkopf, T.; et al. Biomek Cell Workstation. *J. Lab. Autom.* **2016**, *21*, 568–578.
- Lehmann, R.; Gallert, C.; Roddelkopf, T.; et al. 3 Dimensional Cell Cultures: A Comparison between Manually and Automatically Produced Alginate Beads. *Cytotechnology* **2016**, *68*, 1049–1062.
- Lawson, T.; Kehoe, D. E.; Schnitzler, A. C.; et al. Process Development for Expansion of Human Mesenchymal Stromal Cells in a 50L Single-Use Stirred Tank Bioreactor. *Biochem. Eng. J.* **2017**, *120*, 49–62.
- Daniszewski, M.; Crombie, D. E.; Henderson, R.; et al. Automated Cell Culture Systems and Their Applications to Human Pluripotent Stem Cell Studies. *SLAS Technol.* **2018**, *23*, 315–325.
- Iversen, P. W.; Beck, B.; Chen, Y.-F.; et al. HTS Assay Validation. In *Assay Guidance Manual*; Sittampalam, G. S., Grossman, A., Brimacombe, K.; et al., Eds.; Eli Lilly & Company and the National Center for Advancing Translational Sciences: Bethesda, MD, 2012.
- Crombie, D. E.; Daniszewski, M.; Liang, H. H.; et al. Development of a Modular Automated System for Maintenance and Differentiation of Adherent Human Pluripotent Stem Cells. *SLAS Discov.* **2017**, *22*, 1016–1025.
- Czerniecki, S. M.; Cruz, N. M.; Harder, J. L.; et al. High-Throughput Screening Enhances Kidney Organoid Differentiation from Human Pluripotent Stem Cells and Enables Automated Multidimensional Phenotyping. *Cell Stem Cell* **2018**, *22*, 929–940.e4.
- Paull, D.; Sevilla, A.; Zhou, H.; et al. Automated, High-Throughput Derivation, Characterization and Differentiation of Induced Pluripotent Stem Cells. *Nat. Methods* **2015**, *12*, 885–892.
- Hussain, W.; Moens, N.; Veraitch, F. S.; et al. Reproducible Culture and Differentiation of Mouse Embryonic Stem Cells Using an Automated Microwell Platform. *Biochem. Eng. J.* **2013**, *77*, 246–257.
- Kamel, W. A.; Sugihara, E.; Nobusue, H.; et al. Simvastatin-Induced Apoptosis in Osteosarcoma Cells: A Key Role of RhoA-AMPK/p38 MAPK Signaling in Antitumor Activity. *Mol. Cancer Ther.* **2017**, *16*, 182–192.
- Yachie, N.; Robotic Biology Consortium; Natsume, T. Robotic Crowd Biology with Maholo LabDroids. *Nat. Biotechnol.* **2017**, *35*, 310–312.
- Fleischer, H.; Drews, R. R.; Janson, J.; et al. Application of a Dual-Arm Robot in Complex Sample Preparation and Measurement Processes. *J. Lab. Autom.* **2016**, *21*, 671–681.
- Fleischer, H.; Joshi, S.; Roddelkopf, T.; et al. Automated Analytical Measurement Processes Using a Dual-Arm Robotic System. *SLAS Technol.* **2019**, *24*, 354–356.
- Do, H. M.; Choi, T.-Y.; Kyung, J. H. Automation of Cell Production System for Cellular Phones Using Dual-Arm Robots. *Int. J. Adv. Manuf. Technol.* **2016**, *83*, 1349–1360.
- Makris, S.; Tsarouchi, P.; Matthaiakis, A.-S.; et al. Dual Arm Robot in Cooperation with Humans for Flexible Assembly. *CIRP Ann.* **2017**, *66*, 13–16.
- MathWorks. Detect Cell Using Edge Detection and Morphology. <https://jp.mathworks.com/help/images/detecting-a-cell-using-image-segmentation.html?lang=en> (accessed Nov 3, 2020).
- Katiyar, S. K.; Arun, P. V. Comparative Analysis of Common Edge Detection Techniques in Context of Object Extraction. *arXiv*. Preprint posted online Feb 5, 2014. arXiv:1405.6132v1.
- Morisita, M. The Fitting of the Logistic Equation to the Rate of Increase of Population Density. *Res. Popul. Ecol.* **1965**, *7*, 52–55.
- National Institute of Standards and Technology. 4.1.4.3. Weighted Least Squares Regression. <https://www.itl.nist.gov/div898/handbook/pmd/section1/pmd143.htm> (accessed Nov 3, 2020).
- Nelder, J. A.; Mead, R. A Simplex Method for Function Minimization. *Comput. J.* **1965**, *7*, 308–313.
- Kanie, K.; Sasaki, H.; Ikeda, Y.; et al. Quantitative Analysis of Operators’ Flow Line in the Cell Culture for Controlled Manual Operation. *Regen. Ther.* **2019**, *12*, 43–54.